HHS Public Access

Author manuscript

Mucosal Immunol. Author manuscript; available in PMC 2021 September 17.

Published in final edited form as:

Mucosal Immunol. 2021 July ; 14(4): 899–911. doi:10.1038/s41385-021-00388-5.

CD52-targeted depletion by Alemtuzumab ameliorates allergic airway hyperreactivity and lung inflammation

Pedram Shafiei-Jahani, MS[1], **Doumet Georges Helou, PhD**[1], **Benjamin P. Hurrell, PhD**[1], **Lauriane Galle-Treger, PhD**[1], **Emily Howard, BS**[1], **Christine Quach, MS**[1], **Jacob D. Painter, BS**[1], **Marshall Fung, BS**[1], **Richard Lo, MS**[1], **Hooman Allayee, PhD**[2], **Omid Akbari, PhD**[1,*]

[1]Department of Molecular Microbiology and Immunology, Keck School of Medicine, University of Southern California, Los Angeles, California, United States of America.

[2]Department of Preventive Medicine, Keck School of Medicine, University of Southern California, Los Angeles, California.

Abstract

Allergic asthma is a chronic inflammatory disorder associated with airway hyperreactivity (AHR) whose global prevalence is increasing at an alarming rate. Group 2 innate lymphoid cells (ILC2s) and T helper 2 (T_H2) cells are producers of type 2 cytokines, which may contribute to development of AHR. In this study, we explore the potential of CD52-targeted depletion of type 2 immune cells for treating allergic AHR. Here we showed that anti-CD52 therapy can prevent and remarkably reverse established IL-33-induced AHR by reducing airway resistance and alleviating lung inflammation. We further show that CD52 depletion prevents and treats allergic AHR induced by clinically relevant allergens such as *Alternaria alternata* and House Dust Mite (HDM). Importantly, we leverage various humanized mice models of AHR to show new therapeutic applications for Alemtuzumab, an anti-CD52 depleting antibody that is currently FDA-approved for treatment of multiple sclerosis. Our results demonstrate that CD52 depletion is a viable therapeutic option for reduction of pulmonary inflammation, abrogation of eosinophilia, improvement of lung function, and thus treatment of allergic AHR. Taken together, our data suggest that anti-CD52 depleting monoclonal antibodies, such as Alemtuzumab, can serve as viable therapeutic drugs for amelioration of T_H2 and ILC2 dependent AHR.

Keywords

Asthma immunotherapy; Airway hyperreactivity; ILC2; T_H2; CD52; Alemtuzumab

[*]**Corresponding Author**: Omid Akbari, Ph.D., University of Southern California, Keck School of Medicine, Department of Molecular Microbiology and Immunology, NRT 5505, 1450 Biggy St, Los Angeles, California 90033-9605 Tel:323-442-7930 Fax: 323-442-1721. Corresponding: akbari@usc.edu.

Author Contributions: P.S.J. designed, performed and analyzed all experiments and wrote the manuscript, **D.G.H., B.P.H., L.G., E.H., C.Q., J.P., M.F., R.L.** helped perform experiments and provided animal husbandry for experiments. **H.A.** assisted with design and interpretation of data and edited the manuscript. **O.A.** supervised, designed the experiments, conceptualized, interpreted the data and finalized the manuscript. All authors helped with reviewing and editing the manuscript.

Disclosure of potential conflict of interest: The authors have declared that they have no conflict of interest.

INTRODUCTION

Asthma is an atopic and heterogeneous disorder of the airways that is characterized by bronchoconstriction, bronchial hyper-responsiveness and underlying inflammation [1]. Traditionally, asthma has been categorized as an adaptive T_H2 associated inflammatory disorder that is perpetuated by type 2 cytokines, such as IL-5 and IL-13 [2]. These type 2 cytokines stimulate downstream myelocytes such as eosinophils, mast cells and basophils. For instance, IL-5 is essential for recruitment of eosinophils to the lungs from the bone marrow, as well as their respective maturation, growth, activation, and survival [3]. On the other hand, IL-13 causes goblet cell hyperplasia and thus augments production of mucus that causes to the narrowing of the bronchioles [4]. IL-13 can also promote bronchiole smooth muscle contraction by increasing the potency of contractile agonists such as histamine, carbachol, and leukotriene D_4 [56]. Although the adaptive response has been classically implicated in asthma immunopathogenesis, with the entrance of the newly discovered ILC2s into the picture, the exact role of the innate immunity in initiating and perpetuating type 2 immune responses remains to be fully elucidated. Under homeostatic conditions, pulmonary ILC2s reside near the basement membrane subjacent to the epithelium layer at a distance of less than 70 μm away from the bronchioles [7]. Such positioning enables ILC2s to be among the first responders, and thus the earliest inducers of type 2 inflammation in allergic asthma [8]. Similar to T_H2s, ILC2s are very rapid and proficient producers of IL-5 and IL-13 [9]. Thus, ILC2s contribute to pathogenesis of type 2 inflammatory in some groups of allergic asthma [8910]. Due to the vast heterogeneity of asthma and varied contributions of T_H2 and ILC2s in initiating and/or perpetuating lung inflammation in different patients, there has been a growing effort in the field to identify viable biomarkers that can simultaneously target and dampen both ILC2s and T_H2s responses in future therapeutics [8911].

Cluster of differentiation (CD52) is a glycosylphosphatidylinositol (GPI)-anchored cell surface protein that consists of 12 amino acids [12]. Previous reports have suggested CD52 is highly expressed on effector T and B lymphocytes, and to a slighter lower degree on monocytes, mast cells, myeloid-derived dendritic cells, neutrophils, and eosinophils [13–20]. Importantly, CD52 is not expressed on hematopoietic stem cells (HSCs) and other progenitors that give rise to leukocytes [16, 21, 22]. Although its exact physiological function is not yet fully understood, CD52 has shown to be a promising target for several immune system-mediated disease, including multiple sclerosis (MS), graft versus host disease (GvHD), autoimmune inflammatory neurodegenerative diseases, as well as various lymphomas such as chronic lymphocytic leukemia (CLL) or acute lymphocytic leukemia (ALL) [23–27]. In particular, Alemtuzumab is an U.S. Food and Drug Administration (FDA) approved recombinant humanized monoclonal immunoglobulin IgG1 kappa that targets CD52, and is utilized to effectively treat patients with CLL or relapsed-refractory MS [28–33]. The specific role and therapeutic potential of targeting CD52 in allergic asthma has not been previously investigated.

Recently, we reported a genome-wide analysis for 88,486 asthmatic patients and 447,859 healthy controls using data from UK Biobank and the Trans-National Asthma Genetic Consortium [34]. We identified several novel asthma-associated human loci and bioinformatically showed asthma-associated variants of candidate causal genes, such as

CD52, are enriched in regions with open chromatin conformations in T and B cells [34]. Since asthma is a heterogeneous disease, in this study we evaluate the therapeutic potential of anti-CD52 immunotherapy in preventing and treating various models of allergic asthma. We demonstrate that CD52 depletion can severely dampen a T cell driven model of AHR induced by HDM. We further establish CD52 is expressed on both murine and human ILC2s, and show CD52 depletion reduces airway resistance, abrogates eosinophilia and improves dynamic compliance in IL-33-induced AHR in presence and absence of adaptive immunity. We further validate the therapeutic relevance of these findings by demonstrating the therapeutic efficacy of CD52 depletion in *Alternaria alternata*-induced AHR. Lastly, we utilize various humanized mice models to suggest new potential therapeutic applications for the FDA-approved drug Alemtuzumab for treatment of allergic asthma and improvement of lung function.

RESULTS

CD52 depletion ameliorates HDM-induced AHR

We began by asking whether CD52 depletion can prevent induction of airway hyperreactivity (AHR) by house dust mite (HDM), one of the most common triggers behind T cell dependent asthma [35, 36]. We confirmed that CD52 is expressed on T and B cell in our murine model (Supplementary Figure 1). As shown in timeline, wildtype (WT) mice were intraperitoneally (*i.p*) immunized with 100μg of house dust mite (HDM) in 2 mg of aluminum hydroxide and challenged with HDM (50μg) or PBS intranasally (*i.n.*) on days 8, 9 and 10 (Figure 1A). Additionally, mice were treated with 250 μg of anti-CD52 depleting antibody (αCD52) *i.p.* or isotype control on day 7. One day after the last *i.n.* challenge, lung function was measured by direct measurement of lung resistance and dynamic compliance in anesthetized tracheostomized mice, in which mice were mechanically ventilated and sequentially challenged with aerosolized increasing doses of methacholine. After measurements of AHR, the bronchial alveolar lavage (BAL) fluid was collected and analyzed by flow cytometry (Supplementary Figure 2).As expected, *i.n.* administration of HDM significantly increased lung resistance in isotype treated group (Figure 1B); however, lung resistance in αCD52 treated HDM administered group was significantly reduced, indicating that CD52 depletion prevented HDM-induced AHR. In agreement with lung-resistance findings, the results of dynamic compliance showed an improved response in aCD52 treated HDM administered group of mice compared to isotype treated HDM administered group, but they showed a lower dynamic compliance than their PBS treated counterparts (Figure 1C). Moreover, both αCD52 treated and isotype treated mice that received intranasal PBS had similar lung resistance and dynamic compliance. HDM treatment significantly increased the total numbers of $CD45^+$ leukocytes (Figure 1D), eosinophils (Figure 1E), $CD3^+$ T cells (Figure 1F), as well as neutrophils (Figure 1G) in the BAL fluid of isotype treated control. However, BAL analysis in the αCD52 treated HDM administered group revealed a significant reduction in the number of these inflammatory cells, indicating that HDM-induced inflammation is impaired via CD52 depletion (Figures 1, D–G). Additionally, αCD52 treated and isotype treated mice that received intranasal PBS both displayed similar BAL cells numbers, although the numbers of $CD45^+$ and $CD3^+$ were

slightly reduced in the αCD52 treated group. Collectively, these results demonstrate that CD52 depletion effectively prevents HDM-dependent lung inflammation and AHR.

Next, we asked whether CD52 depletion can reverse HDM-induced AHR. A group of WT mice were intraperitoneally immunized with 100αg of HDM in 2 mg of aluminum hydroxide. The mice were then challenged with HDM (50μg) or PBS intranasally (*i.n.*) on days 8, 9 and 10. Subsequently on day 11, mice were treated with 250 μg of anti-CD52 depleting antibody *i.p.* or isotype control. Measurements of lung function and sample acquisition followed on day 13 (Figure 1H). Consistent with the preventative results, CD52 depletion ameliorated established HDM-induced AHR by decreasing lung resistance (Figure 1I) and increasing dynamic compliance (Figure 1J). Furthermore, CD52 depletion effectively abrogated inflammation by reducing the total numbers of $CD45^+$ leukocytes (Figure 1K), eosinophils (Figure 1L), $CD3^+$ T cells (Figure 1M), as well as neutrophils (Figure 1N) in the BAL. In concurrence with the reduction of AHR and eosinophilia in BAL fluid, further histological analyses of the lungs revealed that CD52 depletion decreased airway epithelium thickness and the number of infiltrating cells (Figures 1O). Taken together, these results suggest that anti-CD52 treatment may serve as a novel therapeutic avenue to treat HDM-induced T cell driven allergic AHR.

CD52 is constitutively expressed on murine ILC2s both at steady state and under inflammatory conditions.

Recently, ILC2s have been recognized for their central role in initiating and perpetuating pulmonary inflammation; therefore, we next inquired whether CD52 is expressed on ILC2s. A group of WT mice were challenged with the alarmin IL-33 (0.5 μg) or PBS intranasally (*i.n.*) on days 1, 2 and 3 (Figure 2A). On the fourth day, ILC2s from the lungs were isolated and analyzed by flow cytometry and gated as $lineage^-$ $CD45^+$ $CD127^+$ and $ST2^+$ (Figure 2B). Analysis of pulmonary ILC2s revealed that both naive and IL-33-activated ILC2s (ILC2s stimulated with IL-33) have high expression of CD52 at mRNA (number of transcripts) and protein levels (Figure 2C and D). Furthermore, expression of CD52 on naïve ILC2s is inducible *in vivo* by IL-33 (Figure 2D). In order to determine the kinetics of CD52 induction by IL-33, we next sorted naive ILC2s from a group of WT mice and cultured them in presence of IL-2 and IL-7. The pulmonary ILC2s were subsequently *ex vivo* stimulated with IL-33, and CD52 expression was analyzed overtime at 0, 12, 24, and 48 hours (Figure 2E). We observed that CD52 expression was increased overtime and reached statistical significance after 48 hours of *ex vivo* IL-33 stimulation. Lastly, we demonstrated that expression of CD52 on ILC2s is the highest among the different groups of innate lymphoid cells (Supplementary Figure 3). Overall, these results demonstrate pulmonary murine ILC2s highly express CD52 at both steady-state and under inflammatory conditions.

CD52 depletion ameliorates IL-33-induced AHR in the presence and absence of adaptive immunity

Next, we explored whether CD52 depletion prevent IL-33-induced airway hyperreactivity and lung inflammation by comparing anti-CD52 depleting antibody (αCD52) with isotype treated control in WT mice. The mice were treated with 250 μg of αCD52 *i.p.* or isotype control on day 1. The mice were then challenged with IL-33 (0.5 μg) or PBS intranasally

(*i.n.*) on days 2, 3 and 4 (Figure 3A). On the fifth day lung function was assessed by direct measurement of lung resistance and dynamic compliance in anesthetized tracheostomized mice. After measurements of AHR, the bronchial alveolar lavage fluid was collected and analyzed by flow cytometry. As anticipated, *i.n.* administration of IL-33 significantly increased lung resistance in isotype treated group (Figure 3B); however, lung resistance in αCD52 treated group was significantly reduced, indicating that CD52 depletion prevented IL-33-induced AHR. In agreement with these findings, the results of dynamic compliance showed an improved response in αCD52 treated group of mice compared to isotype control (Figure 3C). Furthermore, αCD52 treated and isotype treated groups that received intranasal PBS displayed similar lung resistance and dynamic compliance. BAL analysis in the αCD52 treated HDM administered group revealed a significant reduction of inflammatory cells. The total number of leukocytes (Figure 3D), T cells (Figure 3E), neutrophils (Figure 3F), and eosinophils (Figure 3G) were abrogated in the BAL of αCD52 treated HDM administered group compared to isotype treated HDM administered mice. Additionally, αCD52 treated and isotype treated mice that received intranasal PBS both displayed similar cells numbers, although the numbers of BAL $CD45^+$ and $CD3^+$ were slightly abrogated in the αCD52 treated group. Importantly, analysis of the lung tissues by flow cytometry revealed the number of pulmonary ILC2s is decreased after αCD52 treatment of HDM administered mice compared to the positive control (Figure 3H), indicating that IL-33-induced inflammation in the lungs of WT mice is curtailed upon CD52 depletion.

Next, we questioned whether the amelioration of IL-33-induced AHR and lung inflammation via CD52 depletion is independent of the adaptive immunity. We examined the effects of anti-CD52 depleting antibody on IL-33-induced AHR and lung inflammation in *Rag2*$^{-/-}$ mice that lacked any mature B and T cells. A group of *Rag2*$^{-/-}$ mice received either anti-CD52 or isotype-matched control antibody (250μg per mouse) intraperitoneally on day 1. The mice were then challenged with IL-33 (0.5 μg) or PBS intranasally on days 2, 3 and 4. Measurements of lung function and sample acquisition followed on day 5 (Figure 3I). Lung function data show that *i.n.* IL-33 administration increased lung resistance (Figure 3J) and decreased dynamic compliance (Figure 3K)in *Rag2*$^{-/-}$ mice. In contrast, lung resistance in IL-33 treated group that received αCD52 was significantly lower, and dynamic compliance was higher, compared to the IL-33 treated isotype-control treated mice (Figure 3 J and K). Furthermore, IL-33 challenge led to eosinophilia (Figure 3L), increased ILC2 numbers (Figure 3M) and thus lung inflammation of the isotype treated group. However, αCD52 treated group showed significantly abrogated inflammatory eosinophil recruitment, and thus reduced eosinophilia in BAL fluid (Figure 3L). Additionally, αCD52 treated group showed a significant decrease in the pulmonary ILC2 numbers (Figure 3M). The secreted amount of IL-5 and IL-13 were similarly decreased in the BAL fluid of αCD52 treated group (Figure 3, N and O). Further histological analysis of the lungs demonstrated that IL-33 challenge led to a thickening of the epithelium and increased inflammatory cells in isotype control but not in the anti-CD52 treated mice (Figure 3P). Taken together, these results indicate anti-CD52 therapy ameliorates ILC2-deriven AHR and lung inflammation in absence of adaptive immunity.

CD52 depletion ameliorates *Alternaria alternata*-induced AHR and reduces lung inflammation in RAG2-deficient mice

We next investigated whether CD52 depletion prevents AHR and lung inflammation induced by a clinically relevant allergen–*Alternaria alternata*–that is known to spark a type 2 innate immune response [37]. *Rag2*$^{-/-}$ mice received either αCD52 or isotype control antibody intraperitoneally on day 1 (250 μg per mouse). The mice were then challenged intranasally with extract of *Alternaria alternata* (100 μg per mouse) or PBS on days 2–6, followed by subsequent measurements of lung function and sample acquisition on day 7 (Figure 4A). Intranasal administration of *Alternaria* induced AHR, as evidenced by increase in lung resistance (Figure 4B) and decrease in dynamic compliance (Figure 4C) in isotype treated mice but not αCD52 treated group. The number of eosinophils was increased in the BAL fluid of *Alternaria* administered mice, but it was significantly ablated in αCD52 treated group compared to the isotype treated control (Figure 4D). Moreover, the total number of ILC2s in the lungs was significantly lowered in αCD52 treated mice compared to the isotype treated group (Figure 4E). Similarly, secreted IL-5 and IL-13 levels were reduced in the αCD52 administered group (Figure 4, F and G). In agreement with the aforementioned results, lung histology revealed an increased thickening of the epithelium layer, as well as an increased number of inflammatory cells in *Alternaria* treated, isotype administered mice but not in *Alternaria* treated, αCD52 administered mice (Figure 4H). Collectively these results show anti-CD52 therapy can prevent *Alternaria alternata*-induced AHR in an ILC2-deriven model of allergic asthma.

We next explored whether CD52 depletion can serve as a therapeutic avenue to reverse established *Alternaria alternata*-induced AHR. A group of *Rag2*$^{-/-}$ mice were challenged intranasally with extract of *Alternaria alternata* (100 μg per mouse) or PBS on days 1–5. Subsequently, the mice received either αCD52 or isotype control antibody intraperitoneally on day 6 (250 μg per mouse). Measurements of lung function and sample acquisition were followed on day 8 (Figure 4I). αCD52 treatment significantly reduced airway resistance (Figure 4J) and increased dynamic compliance (Figure 4K) compared to the isotype control. Furthermore, αCD52 treatment effectively reduced BAL eosinophilia (Figure 4L), and depleted pulmonary ILC2s (Figure 4M). In agreement with the aforementioned findings, the secreted IL-5 (Figure 4N) and IL-13 (Figure 4O) levels were abrogated in the BAL fluid. Collectively, these results demonstrate that CD52 depletion can ameliorate *Alternaria alternata*-induced AHR.

CD52 is expressed on human ILC2s, and its depletion ameliorates human ILC2s-mediated AHR

In order to further validate the translation potential of our findings, we continued to investigate whether human ILC2s express CD52. Human ILC2s were freshly purified from healthy human peripheral blood mononuclear cells and cultured in the presence of both recombinant human IL-2 (rh-IL-2; 10 ng) and IL-7 (rh-IL-7; 10 ng) in the presence or absence of rh-IL-33 (10 ng). Human ILC2s were gated on the basis of the lack of expression of human lineage markers (CD3, CD5, CD14, CD16, CD19, CD20, CD56, CD235a, CD1a, and CD123) and expression of CD45, CRTH2, and CD127 (Figure 5A). CD52 mRNA levels were analyzed after 9 hours of *ex vivo* IL-33 stimulation and revealed CD52 is constitutively

expressed at a mRNA level (Figure 5B). Furthermore, flow cytometry analysis confirmed the protein expression of CD52 after 48 hours of *ex vivo* IL-33 stimulation (Figure 5C). In agreement with aforementioned murine results, CD52 is highly expressed on human circulating ILC2s.

In order to further confirm the translational potential of our findings, we next explored the efficacy of anti-CD52 treatment in ameliorating human ILC2-mediated AHR. We purified ILC2s from human PBMCs of healthy donors and, after 48 hours of *ex vivo* culture in the presence of rh-IL-2 (20 ng/ml) and rh-IL-7 (20 ng/ml), adoptively transferred the human ILC2s through the tail vein to *Rag2*$^{-/-}$*Il2rg*$^{-/-}$ mice, which lack T, B, and NK cells and ILCs. The humanized mice were treated with 250 αg of the FDA-approved anti-human CD52 monoclonal antibody Alemtuzumab (Hu116) *i.p.* or isotype control on day 1, and subsequently challenged with rh-IL-33 (1 αg) or PBS intranasally (*i.n.*) on days 2, 3 and 4 (Figure 5D). On the fifth day we measured lung function as described above and assessed the BAL fluid by flow cytometry. Lung function analysis demonstrated that *i.n.* rh-IL-33 administration increases lung resistance (Figure 5E) and decreases dynamic compliance (Figure 5F) in *Rag2*$^{-/-}$*Il2rg*$^{-/-}$ mice. In contrast, lung resistance in rh-IL-33 treated group that received Alemtuzumab was significantly lower, and dynamic compliance higher, compared to the rh-IL-33 treated isotype-control treated mice (Figure 5, E and F). Furthermore, the rh-IL-33 challenge led to eosinophilia, increased human ILC2 numbers and thus lung inflammation in the recipients of isotype control. However, Alemtuzumab treated group showed significant abrogation of eosinophilia in BAL fluid (Figure 5G). Moreover, Alemtuzumab treated group showed significant depletion and decreased presence of human ILC2s in the lungs (Figure 5H). Taken together, these results indicate that Alemtuzumab depletes human ILC2s *in vivo* and can potentially serve as a novel therapeutic option for amelioration of human ILC2-mediated lung inflammatory diseases. Moreover, since Alemtuzumab only binds and depletes human CD52, these results further indicate CD52-mediated depletion of ILC2s is sufficient for abrogation of AHR.

CD52 depletion ameliorates HDM-induced AHR in preventative and therapeutic humanized models

To further validate the translational potential of our findings in a different humanized model of asthma, we next explored the efficacy of anti-CD52 treatment in HDM-mediated AHR. A group of *Rag2*$^{-/-}$*Il2rg*$^{-/-}$ mice were reconstituted with total peripheral blood mononuclear cells (PBMCs) from HDM-allergic patients on day 0. The humanized mice were then sensitized with HDM on days 3 and 4. The mice were treated with Alemtuzumab or the isotype control (250 μg per mouse) on day 8, and subsequently challenged intranasally with HDM on days 9 to 11. The lung function and BAL fluids were assessed on day 12 (Figure 6A). Interestingly, preventative treatment of recipients with Alemtuzumab significantly improved airway hyperreactivity (Figure 6B) and abrogated eosinophilia in the BAL fluid (Figure 6C). Next, we implemented the Alemtuzumab treatment in a therapeutic humanized model to determine the efficacy of ant-CD52 treatment in reversing established AHR. A group of *Rag2*$^{-/-}$*Il2rg*$^{-/-}$ mice were reconstituted with PBMCs from HDM-allergic patients on day 0 and sensitized intraperitonially on days 3 and 4 (Figure 6D). The humanized mice were challenged intranasally with HDM on days 9, 10 and 11. Subsequently, the humanized

mice were treated with Alemtuzumab or the isotype control (250 μg per mouse) on day 12. The measurements of lung function and analysis of BAL fluid followed on day 14. In agreement with the preventative model, Alemtuzumab treatment ameliorated airway hyperreactivity (Figure 6E), and abrogated BAL eosinophilia (Figure 6F). Taken together, these studies herein demonstrate that CD52 depletion can suppresses AHR in independent models of asthma, and thus crucially suggests a new therapeutic avenue for asthmatic patients.

DISCUSSION

In the present study, we established the therapeutic potential of anti-CD52 immunotherapy in both preventing and reversing AHR and allergic asthma, independent of initiation mechanism. We established that CD52 is expressed on T and B lymphocytes in our AHR model and demonstrated that CD52 depletion can severely lower a T cell driven model of AHR induced by HDM. We further established that CD52 is constitutively expressed by murine and human ILC2s under steady state and inflammatory conditions. Notably, IL-33 enhances CD52 expression in murine ILC2s, but not in human ILC2s. Such dichotomy could be due to the reported biological differences among murine and human ILC2s[38, 39]. Our data also suggest CD52 expression is not inducible on other murine cell types such as T cells and B cells. This observation could be attributed to the unique and distinct biological identities of these immune populations. Subsequently, we established the high efficacy of CD52 depletion for amelioration of IL-33-induced AHR. We utilized an IL-33-based model because both IL-33 and IL-25 have been previously shown to induce ILC2-mediated AHR and lung inflammation, although IL-33 was more potent than IL-25 [40]. In order to exclude the effects of adaptive immune system cells in amelioration of AHR, we utilized *Rag2*$^{-/-}$ mice that lacked any mature B and T cells[41, 42].

Since alarmins, such as IL-33, are not naturally found in the pulmonary environment, we subsequently examined the potential of anti-CD52 treatment on lung inflammation and AHR induced by clinically relevant allergens. In addition to HDM, we utilized *Alternaria alternata* as this allergen has been shown to induce severe allergic AHR in humans [43]. Moreover, Alternaria *alternata* has been reported to cause allergic inflammation in mice independent of adaptive immunity, making it an ideal model to study ILC2-dependent asthma [4445]. Collectively, our result shows depletion of ILC2s and T cells by targeting CD52 improves lung function and curtails lung inflammation following exposure to different principal allergenic agents.

In addition to the CD52-targeted approaches presented in this study, our group and others have previously explored various other tactics for treating allergic asthma by modulation of ILC2 and T cell responses [46–53]. For example, previous studies have recommended direct depletion of CD4$^+$ T_Hs and CD8$^+$ CTLs as a therapeutic avenue for treating asthma; while others have instead suggested targeted depletion of CRTH2$^+$ cells to reduce pulmonary inflammation [5455].These approaches are similar to our presented data as they all result in depletion of T_H2s and ILC2s. Since degranulation of eosinophils is also a key exacerbating event during the autoinflammatory process, others have raised the potential of directly targeting and depleting eosinophils for management of severe asthma [56]. Our results

collectively demonstrate CD52-targeted approach efficiently reduces eosinophilia. Similarly, other groups have highlighted the pathological roles of neutrophils and mast cells, suggesting these cells should be targeted for treatment of asthma [57,58–59]. Our study further establishes CD52-depletion can abrogate the number of neutrophils in the BAL. Myeloid-derived dendritic cells are yet another important population in asthma immunopathogenesis [6061]. Therefore, depletion of this population by a CD52-targeted approach or other similar strategies can have severe therapeutic implications.

Asthma is a complex and heterogeneous disease with different phenotypes and variable manifestations due to participations of multiple types of proinflammatory cells [6263]. As a result, targeting a single cell type may not be sufficient to restore pulmonary tolerance and abrogation of underlying inflammation. There has been a dire need for a viable biological marker, like CD52, that effectively targets all of the pathogenic type 2 populations simultaneously and creates “space in immunity” for reestablishment of peripheral immune tolerance. CD52 is advantageously expressed by all of the aforementioned type 2 immune cells and our results now firmly establish CD52-based therapeutics can ameliorate allergic AHR [162122]. Since HSCs do not express CD52, depletion of $CD52^+$ cells has been shown to be subsequently followed by a gradual repopulation and reprogramming of the immune cells that arise from these stem cell precursors [8,9,64, 65]. Such edited immune profile has been shown to ultimately result in a shift of the immunological networks towards a more tolerogenic state, as evident by the reportedly fast rebound kinetics of regulatory cells such as Tregs [66]. Unlike our CD52-based approach, other asthma therapeutics that target the ubiquitously expressed CD45 are not ideal because they lead to depletion of the HSCs in the bone marrow and thus prevent reconstitution of the immune repertoire without undergoing a bone marrow transplantation [67, 68]. In addition to such therapeutic advantages, our results here introduce powerful amelioration of AHR by CD52-targeted depletion in various models of asthma. Collectively, our results establish depletion of $CD52^+$ cells as a novel strategy for targeting the pathophysiological roots of asthma, ameliorating pulmonary inflammation and AHR, and restoring peripheral immune tolerance to potential treat patients.

It is important to note our results have explored the viability of CD52-targeted therapy for acute models of allergic asthma that do not exhibit lung remodeling. Thus, future investigations are necessary to explore the role and therapeutic effect of anti-CD52 therapy on lung remodeling in chronic models of asthma. Furthermore, we observed a reduction in the number of $CD45^+$ and $CD3^+$ cells in healthy murine models without lung inflammation. Since temporary reduction of these cells can result in short-term partial immune suppression, healthy individuals may be at increased risk of infections and malignancies [65]. Nonetheless, there may still be a population of severe asthmatics with limited therapeutic options [69], such as those with corticosteroid-resistant or eosinophilic asthma, in whom the long-term clinical benefits of anti-CD52 drugs, such as the FDA approved Alemtuzumab, may justify its potential adverse effects. The generally favorable long-term outcomes observed with Alemtuzumab in small numbers of patients with hypereosinophilic syndrome [70, 71] further uphold CD52-targeted treatment as viable concept worthy of further consideration. Moreover, the adverse effects of anti-CD52 treatment could be minimized through careful dosing strategies, such as those used for multiple sclerosis compared to leukemia, and

development of other αCD52 antibodies that may be more efficacious but less immunogenic[72, 73].

In order to further assess the clinical relevance of our findings, we developed various preventative and therapeutic humanized mouse models in which human peripheral ILC2s from healthy donors or PBMCs from HDM-allergic patients are adoptively transferred to *Rag2*$^{-/-}$*Il2rg*$^{-/-}$ mice followed by intranasal administration of either recombinant human IL-33 or HDM to induce AHR and inflammation. Importantly, human IL-5 has been reported to activate murine eosinophils, underscoring the feasibility of using humanized mice in eosinophilic inflammatory studies[74, 75]. As a result, these humanized mouse models provide a unique platform for investigating the contribution of immune cells to human asthma and assessing the efficacy of potential therapeutic targets in preclinical studies. Utilizing this model, we demonstrated that the aforementioned FDA-approved anti-CD52 monoclonal antibody Alemtuzumab efficiently ameliorates both human ILC2 driven and human T_H2 driven AHR by improving lung functions and reducing lung inflammation. Furthermore, our humanized models provided additional insights into the mechanism of anti-CD52 treatment by excluding the direct targeting effect of other murine cells such as $CD52^+$ neutrophils and eosinophils. Alemtuzumab specifically binds and depletes human $CD52^+$ cells only. Thus, our humanized mice results demonstrate specific CD52-target depletion of human ILC2s *in vivo* is sufficient for amelioration of AHR and reduction of mouse eosinophilia. Overall, our humanized models further emphasize the therapeutic potential and translatability of our findings to future clinical studies of asthma.

METHODS

Mice

Wild-type (WT) BALB/cByJ, recombination-activating gene 2-deficient (*Rag2*$^{-/-}$), recombination-activating gene 2-deficient gamma-chain-deficient (*Rag2*$^{-/-}$*Il2rg*$^{-/-}$ mice were purchased from the Jackson Laboratory (Bar Harbor, Me) and bred in our animal facility at the University of Southern California. Mice were maintained at macroenvironmental temperature of 21-22 °C, humidity (48-52%), in a conventional 12:12 light/dark cycle with lights on at 6:00 a.m. and off at 6:00 p.m. We used 5- to 8-week-old age-matched female mice in our studies. All animal studies were approved by the USC institutional Animal Care and Use Committee and conducted in accordance with the USC Department of Animal Resources' guidelines.

Induction and measurement of airway hyperreactivity (AHR) and collection of bronchoalveolar lavage fluid (BALF)

The mice were intranasally challenged via rmIL-33 (BioLegend, San Diego, Calif), *Alternaria alternata* extracts (Greer Laboratories, Lenoir, North Carolina), House Dust Mite (Greer Laboratories, Lenoir, North Carolina), as shown in the experimental schemes. For CD52 depletion, anti-murine CD52 monoclonal antibody (BTG-2G, MBL laboratories) and the corresponding isotypes was used. Lung function was measured by direct measurement of lung resistance and dynamic compliance in anesthetized tracheostomized mice, in which mice were mechanically ventilated via the FinePointe RC system (Buxco Research Systems,

Wilmington, NC) and sequentially challenged with aerosolized increasing doses of methacholine. After measurements of AHR, the trachea was cannulated and the bronchial alveolar lavage (BAL) fluid was collected as described before[76]. Briefly, we tracheostomized and intubated the mice and then washed the airways 3 times with 1 mL of PBS each time, followed by centrifuging at 400g for 7 minutes and harvesting the cells. Data were analyzed with FlowJo software (TreeStar, Ashland, Ore). The levels of IL-5 and IL-13 were measured in BAL using Legendplex multiplex kits (BioLegend) and data were analyzed via the LEGENDplex data analysis software v8.0. The absolute cell numbers in BAL fluid were calculated by means of flow cytometry by staining the cells with phycoerythrin (PE)–anti–Siglec-F (BD Biosciences, San Jose, Calif), fluorescein isothiocyanate(FITC)–anti-CD19, peridinin-chlorophyll-protein complex (PerCP)/Cy5.5–anti-CD3ε, allophycocyanin (APC)–anti–Gr-1, PE/Cy7–anti-CD45, APC/Cy7–anti-CD11c (BioLegend, San Diego, Calif), and eFluor450-anti-CD11b (eBioscience, San Diego, Calif) in the presence of anti-mouse FC-block (BioXcell, West Lebanon, NH). We used CountBright Absolute Count Beads (Thermo Fisher Scientific, Waltham, Mass), according to the manufacturer's instructions. At least 10^5 $CD45^+$ cells were acquired on a BD FACSCanto II (BD Biosciences).

Tissue preparation for flow cytometry

Utilizing fine surgical scissors, murine lungs were surgically removed and minced in a sterile environment subsequently incubated in type IV collagenase (1.6 mg/mL; Worthington Biochemicals, Lakewood, NJ) at 37°C for 60 minutes. After digestion, murine lung fragments were then pressed through a 70 μm nylon cell strainer, using the rubber end of a sterile 10 mL syringe plunger, in order to create a single cell suspension. In order to terminate the enzymatic reaction of collagenase, the cells were washed with 1× phosphate buffered saline (PBS) by centrifugation at 400× g for 7 minutes at 4°C. In order to exclude and lyse the red blood cells (RBCs), the cell pellet was subsequently resuspended in 1× RBC lysis buffer (Biolegend®, San Diego, CA) and incubated at room temperature (RT) for 5 minutes. In order to terminate the chemical reaction, the cells were subsequently washed and centrifuged—at 400× g for 7 minutes at 4°C—with 1× PBS. The remaining pellet was then further prepared for flow cytometry. The absolute cell numbers in lung tissue were calculated by means of flow cytometry. Murine ILC2s were defined based on the lack of expression of classical lineage markers (CD3e, CD5, CD45R, Gr-1, DX5, CD11c, CD11b, Ter119, NK1.1, TCR-γδ and FCεRI) and expression of CD45, ST2, and CD127[41]. Murine ILC1s were defined as lineage negative, ST2 negative, c-Kit negative, CD45 and CD127 positive. Murine ILC3s were defined as lineage negative, ST2 negative, CD45, CD127, and c-Kit positive. All cells were stained with Biotinylated anti-mouse lineage (CD3e (145-2C11), CD5 (53-7.3), CD45R (RA3-3B2), Gr-1 (RB6-8C5), DX5 (DX5), CD11c (N418), CD11b (M1/70), Ter119 (TER-119), NK1.1 (PK136), TCR-b (H57 597), TCR-γδ (GL3), and FcεRIa (MAR-1)), FITC-anti-streptavidin, phycoerythrin (PE)–anti–CD52 (MBL International, Woburn, Massachusetts), APC/Cy7–anti-CD45, PE/Cy7–anti-CD127 (BioLegend, San Diego, Calif), peridinin-chlorophyll-protein complex (PerCP)/Cy5.5–anti-ST2 (Thermo Fisher Scientific, Waltham, Mass), and APC anti-mouse c-Kit (BioLegend, San Diego, Calif). We used CountBright Absolute Count Beads (Thermo Fisher Scientific, Waltham, Mass), according to the manufacturer's instructions. At least 10^5 $CD45^+$ cells

were acquired on a BD FACSCanto II (BD Biosciences). Data were analyzed with FlowJo software (TreeStar, Ashland, Ore).

ex vivo stimulation of ILC2s

All cells were purified by flow cytometry using BD FACS ARIA III (BD biosciences, San Jose, CA) with a purity of >95%. The isolated ILC2s were cultured (at least 5×10^3 cells/well) in 96-well round-bottom plates with Gibco™ Roswell Park Memorial Institute (RPMI) 1640 medium (Thermo Fisher Scientific, Waltham, MA) that was supplemented with 10% fetal bovine serum (FBS), 2% antibiotics (penicillin and streptomycin), and 0.05 mM b-mercaptoethanol. The cells were maintained in a 37°C incubator with 5% CO_2 [77]. All murine ILC2s were cultured in the presence of recombinant mouse rm-IL-2 (10 ng/mL), rm-IL-7 (10 ng/mL), and/or rm-IL-33 (10 ng/mL). All human ILC2s were cultured in the presence of rh-IL-2 (10 ng/mL), rh-IL-7 (10 ng/mL), and/or rh-IL-33 (10 ng/mL).

Isolation of human peripheral blood mononuclear cells (PBMCs) and humanized mice models

All human studies were approved by USC Institutional review board and conducted in accordance to the principles of the Declaration of Helsinki. Informed consent was obtained from all human participants. Human blood samples were obtained from male and female healthy donors (Age 18 to 65). In few experiments, blood was collected from allergic patients having positive skin tests to house dust mite antigen. Informed consent was obtained from all subjects according to our approved IRB protocols. Peripheral blood mononuclear cells (PBMCs) from donors were first isolated from fresh blood by diluting the blood 1:1 in PBS then adding to SepMateTM-50 separation tubes (STEMCELL Technologies Inc, Vancouver, Canada) prefilled with 15-ml LymphoprepTM each (Axis-Shield, Oslo, Norway) and centrifugation at 1200 ×g for 15 minutes. Human PBMCs were then stained and purified using BD FACS ARIA III (BD Biosciences, San Jose, CA) with a purity of 95%. Human ILC2s were defined based on the lack of expression of classical human lineage markers and expression of CRTH2, CD127 and CD45. The cells were stained with fluorescein isothiocyanate(FITC)–anti-human lineage (CD3, CD5, CD14, CD16, CD19, CD20, CD56, CD235a, CD1a, CD123), APC/Cy7–anti-CD45, phycoerythrin (PE)–anti–CD294 (CRTH2), PE/Cy7–anti-CD127, allophycocyanin (APC)–anti–CD52 (BioLegend, San Diego, Calif). We used CountBright Absolute Count Beads (Thermo Fisher Scientific, Waltham, Mass), according to the manufacturer's instructions. At least 10^5 $CD45^+$ cells were acquired on a BD FACSCanto II (BD Biosciences). Data were analyzed with FlowJo software (TreeStar, Ashland, Ore). For some experiments, purified human ILC2s were cultured with recombinant human (rh)-IL-2 (20 $ng.ml^{-1}$) and rh-IL-7 (20 $ng.ml^{-1}$) for 48 hours, then adoptively transferred to *Rag2*$^{-/-}$*Il2rg*$^{-/-}$ mice (2.5×10^5 ILC2s per mouse). For some experiments, 5 million PBMCs were adoptively transferred to *Rag2*$^{-/-}$*Il2rg*$^{-/-}$ mice [78]. The humanized mice were challenged *i.n.* via 1 μg of rh-IL-33 (BioLegend, San Diego, Calif) or House Dust Mite (Greer Laboratories, Lenoir, North Carolina). Alemtuzumab (Hu116) or the isotype control were purchased from R&D Systems.

Histological Analysis of the Lungs

The lungs were injected and fixed with 10% paraformaldehyde in PBS until inflated as described before [79]. After overnight fixation, the lungs were processed for histology as described before [79]. The lung tissue was embedded in paraffin, cut into 4 μm sections and stained with H&E according to standard protocols [49, 51]. Sections were scanned using light microscope for inflammation. Images of hematoxylin and eosin–stained tissue slides were acquired with a KeyenceBZ-9000 microscope (Keyence, Itasca, Ill) and assembled into multipanel figures using Adobe Illustrator software (version 22.1). Histologic images were analyzed per user guide with the ImageJ Analysis Application (NIH & LOCI, University of Wisconsin) and quantified results were presented as demonstrated before [49, 51]. Briefly, acquired Images of hematoxylin and eosin–stained tissue were saved as high resolution TIFF files. Subsequently, we measured the epithelium thickness of each individual airway in 8 randomly selected segments. This process was repeated for 6 different airways in each animal and the representative epithelial thickness for each mouse was then quantified by averaging these obtained measurements. For quantification of the cell number, 8 random representative sites of the same area (250 μm^2) for each mouse were selected, cells were enumerated in each site, and the average of the number of cells per site was calculated and presented as the representative value for each mouse.

Statistical Analysis

All data are expressed as mean ± standard error of the mean (SEM). Comparisons between study groups were analyzed by Student's t-tests and one-way ANOVA by Tukey post-hoc tests. P values of <0.05 were considered to be statistically significant. Statistical analyses were performed using the GraphPad Prism 7 software (La Jolla, CA).

Supplementary Material

Refer to Web version on PubMed Central for supplementary material.

Acknowledgments:

This article was financially supported by National Institutes of Health Public Health Service grants R01 ES025786, R01 ES021801, R01 HL151493, R01 HL144790, R01 AI145813, R21 AI132084 (O.A.).

REFERENCES

1. National Asthma E, Prevention P. Expert Panel Report 3 (EPR-3): Guidelines for the Diagnosis and Management of Asthma-Summary Report 2007. J Allergy Clin Immunol 2007; 120(5 Suppl): S94–138. [PubMed: 17983880]
2. Fahy JV. Type 2 inflammation in asthma--present in most, absent in many. Nat Rev Immunol 2015; 15(1): 57–65. [PubMed: 25534623]
3. McBrien CN, Menzies-Gow A. The Biology of Eosinophils and Their Role in Asthma. Front Med (Lausanne) 2017; 4: 93. [PubMed: 28713812]
4. Maazi H, Akbari O. Type two innate lymphoid cells: the Janus cells in health and disease. Immunol Rev 2017; 278(1): 192–206. [PubMed: 28658553]
5. Russo A, Ranieri M, Di Mise A, Dossena S, Pellegrino T, Furia E et al. Interleukin-13 increases pendrin abundance to the cell surface in bronchial NCI-H292 cells via Rho/actin signaling. Pflugers Arch 2017; 469(9): 1163–1176. [PubMed: 28378089]

6. Manson ML, Safholm J, James A, Johnsson AK, Bergman P, Al-Ameri M et al. IL-13 and IL-4, but not IL-5 nor IL-17A, induce hyperresponsiveness in isolated human small airways. J Allergy Clin Immunol 2020; 145(3): 808–817 e802. [PubMed: 31805312]
7. Sui P, Wiesner DL, Xu J, Zhang Y, Lee J, Van Dyken S et al. Pulmonary neuroendocrine cells amplify allergic asthma responses. Science 2018; 360(6393).
8. Hurrell BP, Shafiei Jahani P, Akbari O. Social Networking of Group Two Innate Lymphoid Cells in Allergy and Asthma. Front Immunol 2018; 9: 2694. [PubMed: 30524437]
9. Lambrecht BN, Hammad H. The immunology of asthma. Nat Immunol 2015; 16(1): 45–56. [PubMed: 25521684]
10. Kuruvilla ME, Lee FE, Lee GB. Understanding Asthma Phenotypes, Endotypes, and Mechanisms of Disease. Clin Rev Allergy Immunol 2019; 56(2): 219–233. [PubMed: 30206782]
11. Dunican EM, Fahy JV. The Role of Type 2 Inflammation in the Pathogenesis of Asthma Exacerbations. Ann Am Thorac Soc 2015; 12 Suppl 2: S144–149. [PubMed: 26595730]
12. James LC, Hale G, Waldmann H, Bloomer AC. 1.9 A structure of the therapeutic antibody CAMPATH-1H fab in complex with a synthetic peptide antigen. J Mol Biol 1999; 289(2): 293–301. [PubMed: 10366506]
13. Ratzinger G, Reagan JL, Heller G, Busam KJ, Young JW. Differential CD52 expression by distinct myeloid dendritic cell subsets: implications for alemtuzumab activity at the level of antigen presentation in allogeneic graft-host interactions in transplantation. Blood 2003; 101(4): 1422–1429. [PubMed: 12393688]
14. Buggins AG, Mufti GJ, Salisbury J, Codd J, Westwood N, Arno M et al. Peripheral blood but not tissue dendritic cells express CD52 and are depleted by treatment with alemtuzumab. Blood 2002; 100(5): 1715–1720. [PubMed: 12176892]
15. Osuji N, Del Giudice I, Matutes E, Morilla A, Owusu-Ankomah K, Morilla R et al. CD52 expression in T-cell large granular lymphocyte leukemia--implications for treatment with alemtuzumab. Leuk Lymphoma 2005; 46(5): 723–727. [PubMed: 16019510]
16. Ginaldi L, De Martinis M, Matutes E, Farahat N, Morilla R, Dyer MJ et al. Levels of expression of CD52 in normal and leukemic B and T cells: correlation with in vivo therapeutic responses to Campath-1H. Leuk Res 1998; 22(2): 185–191. [PubMed: 9593475]
17. Ambrose LR, Morel AS, Warrens AN. Neutrophils express CD52 and exhibit complement-mediated lysis in the presence of alemtuzumab. Blood 2009; 114(14): 3052–3055. [PubMed: 19638623]
18. Zhang PL, Pennington JR, Prichard JW, Blasick TM, Brown AM, Potdar S. CD52 antigen may be a therapeutic target for eosinophilic rhinosinusitis. Ann Clin Lab Sci 2007; 37(2): 148–151. [PubMed: 17522370]
19. Jiang L, Yuan CM, Hubacheck J, Janik JE, Wilson W, Morris JC et al. Variable CD52 expression in mature T cell and NK cell malignancies: implications for alemtuzumab therapy. Br J Haematol 2009; 145(2): 173–179. [PubMed: 19236377]
20. Santos DD, Hatjiharissi E, Tournilhac O, Chemaly MZ, Leleu X, Xu L et al. CD52 is expressed on human mast cells and is a potential therapeutic target in Waldenstrom's Macroglobulinemia and mast cell disorders. Clin Lymphoma Myeloma 2006; 6(6): 478–483. [PubMed: 16796779]
21. Rodig SJ, Abramson JS, Pinkus GS, Treon SP, Dorfman DM, Dong HY et al. Heterogeneous CD52 expression among hematologic neoplasms: implications for the use of alemtuzumab (CAMPATH-1H). Clin Cancer Res 2006; 12(23): 7174–7179. [PubMed: 17145843]
22. Hale G The CD52 antigen and development of the CAMPATH antibodies. Cytotherapy 2001; 3(3): 137–143. [PubMed: 12171721]
23. Kalincik T, Brown JWL, Robertson N, Willis M, Scolding N, Rice CM et al. Treatment effectiveness of alemtuzumab compared with natalizumab, fingolimod, and interferon beta in relapsing-remitting multiple sclerosis: a cohort study. Lancet Neurol 2017; 16(4): 271–281. [PubMed: 28209331]
24. Vojdeman FJ, Herman SEM, Kirkby N, Wiestner A, van T' Veer MB, Tjonnfjord GE et al. Soluble CD52 is an indicator of disease activity in chronic lymphocytic leukemia. Leuk Lymphoma 2017; 58(10): 2356–2362. [PubMed: 28278728]

25. Ishizawa K, Fukuhara N, Nakaseko C, Chiba S, Ogura M, Okamoto A et al. Safety, efficacy and pharmacokinetics of humanized anti-CD52 monoclonal antibody alemtuzumab in Japanese patients with relapsed or refractory B-cell chronic lymphocytic leukemia. Jpn J Clin Oncol 2017; 47(1): 54–60. [PubMed: 28122892]
26. Ravandi F, O'Brien S. Alemtuzumab in CLL and other lymphoid neoplasms. Cancer Invest 2006; 24(7): 718–725. [PubMed: 17118783]
27. van der Zwan M, Baan CC, van Gelder T, Hesselink DA. Review of the Clinical Pharmacokinetics and Pharmacodynamics of Alemtuzumab and Its Use in Kidney Transplantation. Clin Pharmacokinet 2018; 57(2): 191–207. [PubMed: 28669130]
28. Zhang J, Shi S, Zhang Y, Luo J, Xiao Y, Meng L et al. Alemtuzumab versus interferon beta 1a for relapsing-remitting multiple sclerosis. Cochrane Database Syst Rev 2017; 11: CD010968. [PubMed: 29178444]
29. Giovannoni G, Cohen JA, Coles AJ, Hartung HP, Havrdova E, Selmaj KW et al. Alemtuzumab improves preexisting disability in active relapsing-remitting MS patients. Neurology 2016; 87(19): 1985–1992. [PubMed: 27733571]
30. Riera R, Porfirio GJ, Torloni MR. Alemtuzumab for multiple sclerosis. Cochrane Database Syst Rev 2016; 4: CD011203. [PubMed: 27082500]
31. Al-Sawaf O, Fischer K, Herling CD, Ritgen M, Bottcher S, Bahlo J et al. Alemtuzumab consolidation in chronic lymphocytic leukaemia: a phase I/II multicentre trial. Eur J Haematol 2017; 98(3): 254–262. [PubMed: 27862308]
32. Smolej L, Prochazka V, Spacek M, Obrtlikova P, Gumulec J, Vokurka S et al. [Guidelines for alemtuzumab treatment in chronic lymphocytic leukaemia (CLL)]. Vnitr Lek 2012; 58(3): 232–236. [PubMed: 22486291]
33. Alinari L, Lapalombella R, Andritsos L, Baiocchi RA, Lin TS, Byrd JC. Alemtuzumab (Campath-1H) in the treatment of chronic lymphocytic leukemia. Oncogene 2007; 26(25): 3644–3653. [PubMed: 17530018]
34. Han Y, Jia Q, Jahani PS, Hurrell BP, Pan C, Huang P et al. Genome-wide analysis highlights contribution of immune system pathways to the genetic architecture of asthma. Nat Commun 2020; 11(1): 1776. [PubMed: 32296059]
35. Fassio F, Guagnini F. House dust mite-related respiratory allergies and probiotics: a narrative review. Clin Mol Allergy 2018; 16: 15. [PubMed: 29946225]
36. Gregory LG, Lloyd CM. Orchestrating house dust mite-associated allergy in the lung. Trends Immunol 2011; 32(9): 402–411. [PubMed: 21783420]
37. Bartemes KR, Kita H. Innate and adaptive immune responses to fungi in the airway. J Allergy Clin Immunol 2018; 142(2): 353–363. [PubMed: 30080527]
38. Mazzurana L, Rao A, Van Acker A, Mjosberg J. The roles for innate lymphoid cells in the human immune system. Semin Immunopathol 2018; 40(4): 407–419. [PubMed: 29948108]
39. Guia S, Narni-Mancinelli E. Helper-like Innate Lymphoid Cells in Humans and Mice. Trends Immunol 2020; 41(5): 436–452. [PubMed: 32223931]
40. Barlow JL, Peel S, Fox J, Panova V, Hardman CS, Camelo A et al. IL-33 is more potent than IL-25 in provoking IL-13-producing nuocytes (type 2 innate lymphoid cells) and airway contraction. J Allergy Clin Immunol 2013; 132(4): 933–941. [PubMed: 23810766]
41. Shafiei-Jahani P, Hurrell BP, Galle-Treger L, Helou DG, Howard E, Painter J et al. DR3 stimulation of adipose resident ILC2s ameliorates type 2 diabetes mellitus. Nat Commun 2020; 11(1): 4718. [PubMed: 32948777]
42. Sadofsky MJ. The RAG proteins in V(D)J recombination: more than just a nuclease. Nucleic Acids Res 2001; 29(7): 1399–1409. [PubMed: 11266539]
43. Salo PM, Arbes SJ Jr., Sever M, Jaramillo R, Cohn RD, London SJ et al. Exposure to Alternaria alternata in US homes is associated with asthma symptoms. J Allergy Clin Immunol 2006; 118(4): 892–898. [PubMed: 17030243]
44. Karta MR, Rosenthal PS, Beppu A, Vuong CY, Miller M, Das S et al. beta2 integrins rather than beta1 integrins mediate Alternaria-induced group 2 innate lymphoid cell trafficking to the lung. J Allergy Clin Immunol 2018; 141(1): 329–338 e312. [PubMed: 28366795]

45. Kim HK, Lund S, Baum R, Rosenthal P, Khorram N, Doherty TA. Innate type 2 response to Alternaria extract enhances ryegrass-induced lung inflammation. Int Arch Allergy Immunol 2014; 163(2): 92–105. [PubMed: 24296722]
46. Galle-Treger L, Hurrell BP, Lewis G, Howard E, Jahani PS, Banie H et al. Autophagy is critical for group 2 innate lymphoid cell metabolic homeostasis and effector function. J Allergy Clin Immunol 2020; 145(2): 502–517 e505. [PubMed: 31738991]
47. Hurrell BP, Galle-Treger L, Jahani PS, Howard E, Helou DG, Banie H et al. TNFR2 Signaling Enhances ILC2 Survival, Function, and Induction of Airway Hyperreactivity. Cell Rep 2019; 29(13): 4509–4524 e4505. [PubMed: 31875557]
48. Hurrell BP, Howard E, Galle-Treger L, Helou DG, Shafiei-Jahani P, Painter JD et al. Distinct Roles of LFA-1 and ICAM-1 on ILC2s Control Lung Infiltration, Effector Functions, and Development of Airway Hyperreactivity. Front Immunol 2020; 11: 542818. [PubMed: 33193309]
49. Maazi H, Patel N, Sankaranarayanan I, Suzuki Y, Rigas D, Soroosh P et al. ICOS:ICOS-ligand interaction is required for type 2 innate lymphoid cell function, homeostasis, and induction of airway hyperreactivity. Immunity 2015; 42(3): 538–551. [PubMed: 25769613]
50. Maazi H, Banie H, Aleman Muench GR, Patel N, Wang B, Sankaranarayanan I et al. Activated plasmacytoid dendritic cells regulate type 2 innate lymphoid cell-mediated airway hyperreactivity. J Allergy Clin Immunol 2018; 141(3): 893–905 e896. [PubMed: 28579374]
51. Galle-Treger L, Suzuki Y, Patel N, Sankaranarayanan I, Aron JL, Maazi H et al. Nicotinic acetylcholine receptor agonist attenuates ILC2-dependent airway hyperreactivity. Nat Commun 2016; 7: 13202. [PubMed: 27752043]
52. Rigas D, Lewis G, Aron JL, Wang B, Banie H, Sankaranarayanan I et al. Type 2 innate lymphoid cell suppression by regulatory T cells attenuates airway hyperreactivity and requires inducible T-cell costimulator-inducible T-cell costimulator ligand interaction. J Allergy Clin Immunol 2017; 139(5): 1468–1477 e1462. [PubMed: 27717665]
53. Suzuki Y, Maazi H, Sankaranarayanan I, Lam J, Khoo B, Soroosh P et al. Lack of autophagy induces steroid-resistant airway inflammation. J Allergy Clin Immunol 2016; 137(5): 1382–1389 e1389. [PubMed: 26589586]
54. Raemdonck K, Baker K, Dale N, Dubuis E, Shala F, Belvisi MG et al. CD4(+) and CD8(+) T cells play a central role in a HDM driven model of allergic asthma. Respir Res 2016; 17: 45. [PubMed: 27112462]
55. Huang T, Hazen M, Shang Y, Zhou M, Wu X, Yan D et al. Depletion of major pathogenic cells in asthma by targeting CRTh2. JCI Insight 2016; 1(7): e86689. [PubMed: 27699264]
56. Matsuno O, Minamoto S. Eosinophils depletion therapy for severe asthma management following favorable response to mepolizumab. Respir Med Case Rep 2019; 28: 100899. [PubMed: 31341763]
57. Gao H, Ying S, Dai Y. Pathological Roles of Neutrophil-Mediated Inflammation in Asthma and Its Potential for Therapy as a Target. J Immunol Res 2017; 2017: 3743048. [PubMed: 29359169]
58. Ray A, Kolls JK. Neutrophilic Inflammation in Asthma and Association with Disease Severity. Trends Immunol 2017; 38(12): 942–954. [PubMed: 28784414]
59. Mendez-Enriquez E, Hallgren J. Mast Cells and Their Progenitors in Allergic Asthma. Front Immunol 2019; 10: 821. [PubMed: 31191511]
60. Gaurav R, Agrawal DK. Clinical view on the importance of dendritic cells in asthma. Expert Rev Clin Immunol 2013; 9(10): 899–919. [PubMed: 24128155]
61. Vroman H, Hendriks RW, Kool M. Dendritic Cell Subsets in Asthma: Impaired Tolerance or Exaggerated Inflammation? Front Immunol 2017; 8: 941. [PubMed: 28848549]
62. Howard E, Lewis G, Galle-Treger L, Hurrell BP, Helou DG, Shafiei-Jahani P et al. IL-10 production by ILC2s requires Blimp-1 and cMaf, modulates cellular metabolism, and ameliorates airway hyperreactivity. J Allergy Clin Immunol 2020.
63. Carr TF, Bleecker E. Asthma heterogeneity and severity. World Allergy Organ J 2016; 9(1): 41. [PubMed: 27980705]
64. Wiendl H, Kieseier B. Multiple sclerosis: reprogramming the immune repertoire with alemtuzumab in MS. Nat Rev Neurol 2013; 9(3): 125–126. [PubMed: 23358486]

65. Ruck T, Bittner S, Wiendl H, Meuth SG. Alemtuzumab in Multiple Sclerosis: Mechanism of Action and Beyond. Int J Mol Sci 2015; 16(7): 16414–16439. [PubMed: 26204829]
66. Jones JL, Thompson SA, Loh P, Davies JL, Tuohy OC, Curry AJ et al. Human autoimmunity after lymphocyte depletion is caused by homeostatic T-cell proliferation. Proc Natl Acad Sci U S A 2013; 110(50): 20200–20205. [PubMed: 24282306]
67. Shivtiel S, Kollet O, Lapid K, Schajnovitz A, Goichberg P, Kalinkovich A et al. CD45 regulates retention, motility, and numbers of hematopoietic progenitors, and affects osteoclast remodeling of metaphyseal trabecules. J Exp Med 2008; 205(10): 2381–2395. [PubMed: 18779349]
68. Hermiston ML, Xu Z, Weiss A. CD45: a critical regulator of signaling thresholds in immune cells. Annu Rev Immunol 2003; 21: 107–137. [PubMed: 12414720]
69. Canonica GW, Senna G, Mitchell PD, O'Byrne PM, Passalacqua G, Varricchi G. Therapeutic interventions in severe asthma. World Allergy Organ J 2016; 9(1): 40. [PubMed: 27942351]
70. Wechsler ME, Fulkerson PC, Bochner BS, Gauvreau GM, Gleich GJ, Henkel T et al. Novel targeted therapies for eosinophilic disorders. J Allergy Clin Immunol 2012; 130(3): 563–571. [PubMed: 22935585]
71. Strati P, Cortes J, Faderl S, Kantarjian H, Verstovsek S. Long-term follow-up of patients with hypereosinophilic syndrome treated with Alemtuzumab, an anti-CD52 antibody. Clin Lymphoma Myeloma Leuk 2013; 13(3): 287–291. [PubMed: 23123105]
72. Havrdova E, Horakova D, Kovarova I. Alemtuzumab in the treatment of multiple sclerosis: key clinical trial results and considerations for use. Ther Adv Neurol Disord 2015; 8(1): 31–45. [PubMed: 25584072]
73. Holgate RG, Weldon R, Jones TD, Baker MP. Characterisation of a Novel Anti-CD52 Antibody with Improved Efficacy and Reduced Immunogenicity. PLoS One 2015; 10(9): e0138123. [PubMed: 26372145]
74. Ingley E, Cutler RL, Fung MC, Sanderson CJ, Young IG. Production and purification of recombinant human interleukin-5 from yeast and baculovirus expression systems. Eur J Biochem 1991; 196(3): 623–629. [PubMed: 2013285]
75. Tavernier J, Tuypens T, Verhee A, Plaetinck G, Devos R, Van der Heyden J et al. Identification of receptor-binding domains on human interleukin 5 and design of an interleukin 5-derived receptor antagonist. Proc Natl Acad Sci U S A 1995; 92(11): 5194–5198. [PubMed: 7761472]
76. Maazi H, Singh AK, Speak AO, Lombardi V, Lam J, Khoo B et al. Lack of PD-L1 expression by iNKT cells improves the course of influenza A infection. PLoS One 2013; 8(3): e59599. [PubMed: 23555047]
77. Hirose S, Jahani PS, Wang S, Jaggi U, Tormanen K, Yu J et al. Type 2 Innate Lymphoid Cells Induce CNS Demyelination in an HSV-IL-2 Mouse Model of Multiple Sclerosis, iScience 2020 23(10): 101549. [PubMed: 33083718]
78. Helou DG, Shafiei-Jahani P, Lo R, Howard E, Hurrell BP, Galle-Treger L et al. PD-1 pathway regulates ILC2 metabolism and PD-1 agonist treatment ameliorates airway hyperreactivity. Nat Commun 2020; 11(1): 3998. [PubMed: 32778730]
79. Morton J, Snider TA. Guidelines for collection and processing of lungs from aged mice for histological studies. Pathobiol Aging Age Relat Dis 2017; 7(1): 1313676. [PubMed: 28515862]

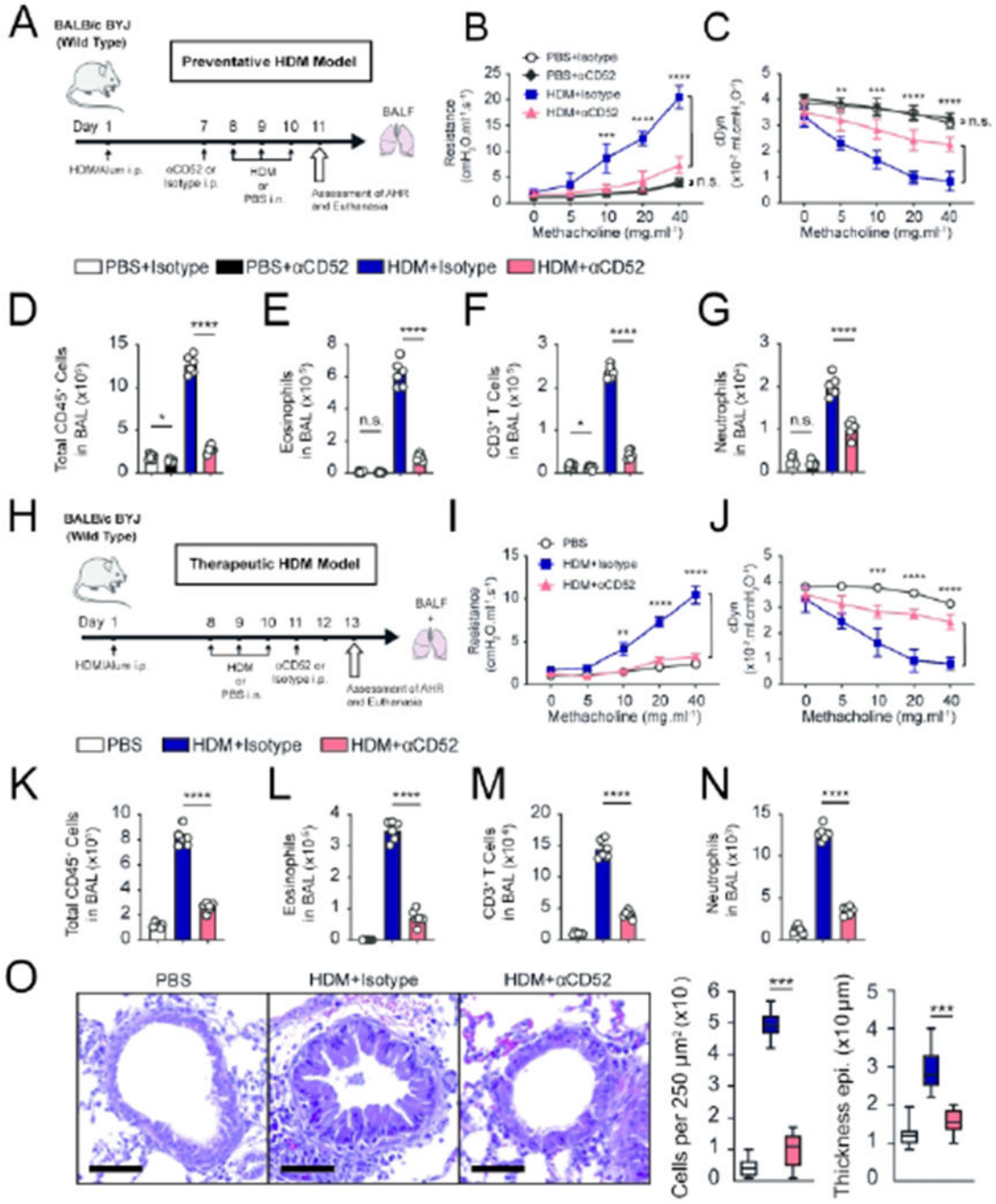

Figure 1. CD52 depletion ameliorates HDM-induced airway hyperreactivity (AHR) and abrogates inflammation.

A, A group of WT mice (n=6 mice) were intraperitoneally (*i.p*) immunized with 100µg of house dust mite (HDM) in 2 mg of aluminum hydroxide (alum) and challenged with HDM (50µg) or PBS intranasally (*i.n.*) on days 8, 9 and 10. Mice were treated with 250µg of anti-CD52 depleting antibody (αCD52) *i.p.* or isotype control on day 7. We assessed the lung function and analyzed the BAL fluid on day 11, as shown in the timeline. **B** and **C,** line graph show lung resistance and dynamic compliance (cDyn) in response to increasing doses

of methacholine. Total numbers of $CD45^+$ cells (**D**), number of eosinophils **(E),** number of T cells **(F),** and number of neutrophils **(G)** in the BAL fluid have been demonstrated in the bar graphs. **H,** WT mice (n=6 mice) were sensitized on day 1, and challenged intranasally with HDM on days 8, 9 and 10. Subsequently, the mice were treated with 250μg of αCD52 or isotype control. The lung function and BAL were assessed on day 13. **I,** lung resistance. **J,** dynamic compliance. **K,** total numbers of $CD45^+$ cells. **L,** number of eosinophils. **M,** number of T cells. **N,** number of neutrophils. **E,** Representative images (left panel) and quantification (right panel) of hematoxylin and eosin–stained histologic sections of the lungs of mice. Scale bars=50 μm. Data are shown as means ± SEMs and are representative of 3 individual experiments. Statistical analysis, two-tailed student's t-test; n.s., not significant, *P < .05, **P < .01, ***P < .001, ****P < .0001. Mouse and lung images are provided with permission from Servier Medical Art.

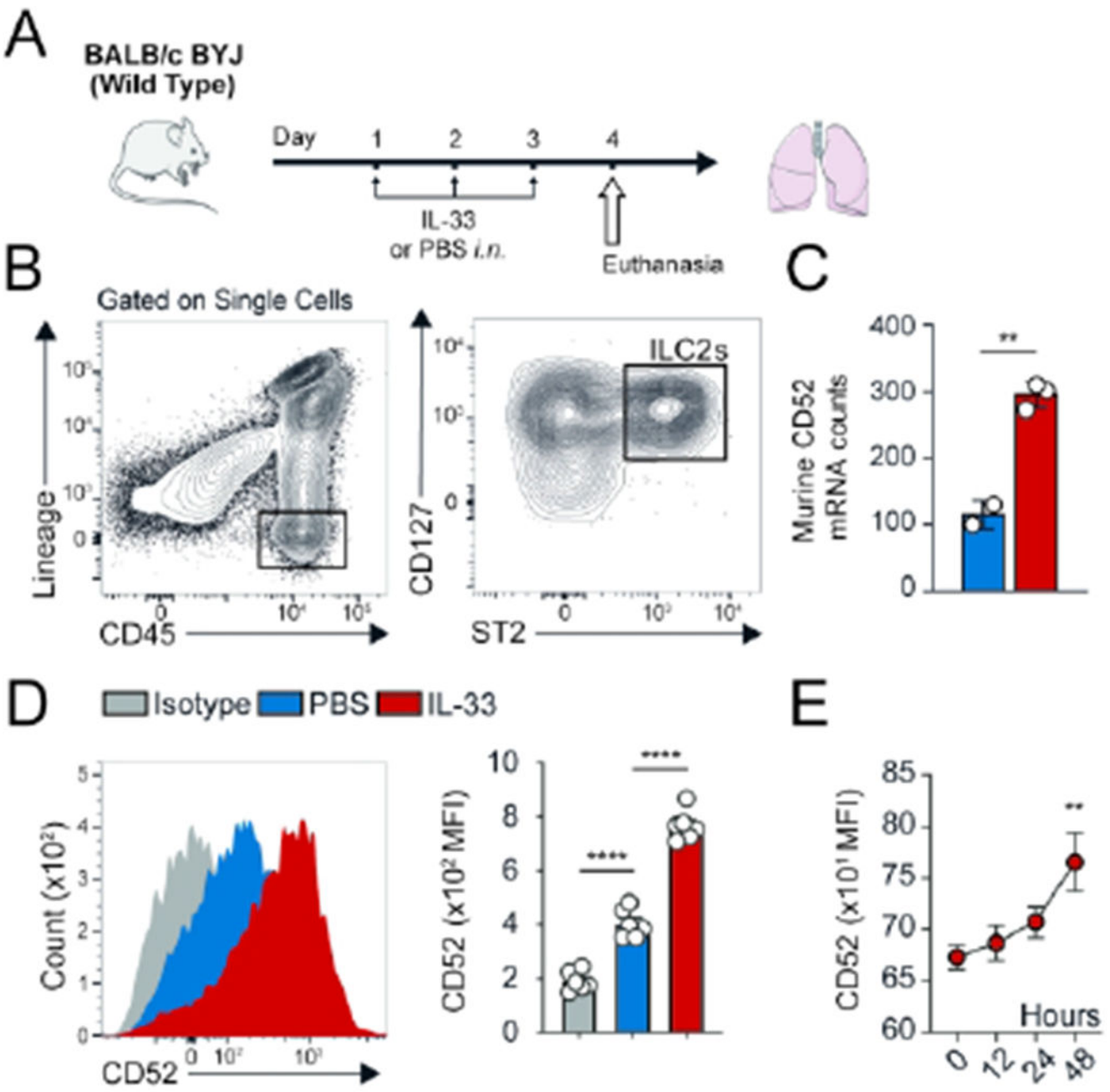

Figure 2. Murine ILC2s constitutively express CD52, and this expression is inducible by IL-33.

A, A group of WT mice (n=6 mice) were challenged with recombinant mouse (rm)-IL-33 (0.5 μg in 50 μL) or PBS intranasally (*i.n.*) on days 1, 2 and 3. The mice were euthanized on day 4 and the lung was isolated, as shown in the timeline. **B,** The gating strategy of ILC2s identified as $Lin^{-}CD45^{+}CD127^{+}ST2^{+}$ cells. **C** and **D**, mRNA and protein expression levels of CD52 in both naive (PBS) and IL-33-activated ILC2s in the lungs. Corresponding FACS quantitation of CD52 expression shown as MFI+/− SEM, n = 6 mice. mRNA levels obtained from n=2-3 mice. **E**, Naïve pulmonary ILC2s were sorted (n=6 mice) and subsequently cultured with rm-IL-2 and rm-IL-7 and rm-IL-33 for 12, 24, and 48 hours. Freshly isolated

ILC2s at 0 hours and *ex vivo* activated ILC2s were analyzed by flow cytometry as indicated in the scheme and the kinetics of CD52 induction by IL-33 is shown. Statistical analysis, two-tailed student's t-test or one-way ANOVA followed by Tukey post-hoc tests; **P < .01, ***P < .001. Mouse and lung images are provided with permission from Servier Medical Art.

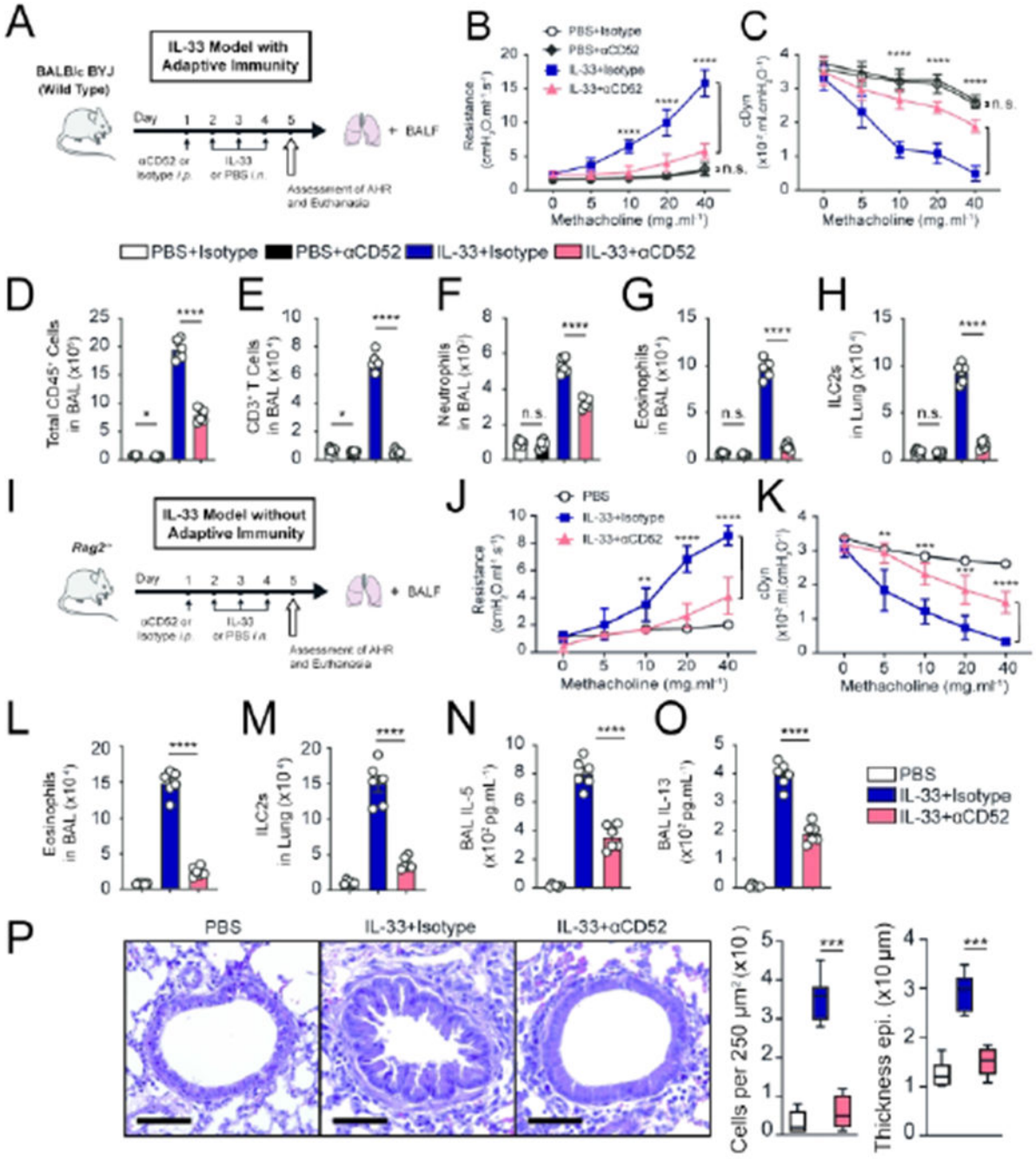

Figure 3. CD52 depletion significantly ameliorates IL-33-induced AHR and pulmonary inflammation.

A, A group of WT mice (n=6 mice) were treated with 250μg of anti-CD52 depleting antibody (αCD52) *i.p.* or isotype control on day 1. Additionally, the mice were challenged with recombinant mouse (rm)-IL-33 (0.5μg) or PBS intranasally (*i.n.*) on days 2, 3 and 4. On day 5, we assessed the lung function and acquired the samples, as shown in the timeline. **B** and **C,** Line graph show lung resistance and dynamic compliance (cDyn) in response to increasing doses of methacholine. Total numbers of $CD45^+$ cells (**D**), $CD3^+$ T cells (**E**),

neutrophils (**F**), and eosinophils **(G)** in BAL fluid have been demonstrated in the bar graphs. **H,** the numbers of ILC2s in the lungs. **I,** *Rag2*$^{-/-}$ mice (n=6 mice) were treated with 250μg of αCD52 *i.p.* or isotype control on day 1, and subsequently challenged with rm-IL-33 (0.5μg) or PBS *i.n.* on days 2, 3 and 4. The lung function and samples were measured on day 5. **J,** lung resistance. **K,** dynamic compliance. **L,** number of eosinophils in BAL fluid. **M,** number of ILC2s in lungs. **N,** IL-5 levels in BAL. **O,** IL-13 levels in BAL. **P,** representative images (left panel) and quantification (right panel) of hematoxylin and eosin-stained histologic sections of the lungs of mice. Scale bars=50 μm. Data are shown as means ± SEMs and are representative of 3 individual experiments. Statistical analysis, two-tailed student's t-test; n.s., not significant, *P < .05, **P < .01, ***P < .001, ****p < .0001. Mouse and lung images are provided with permission from Servier Medical Art.

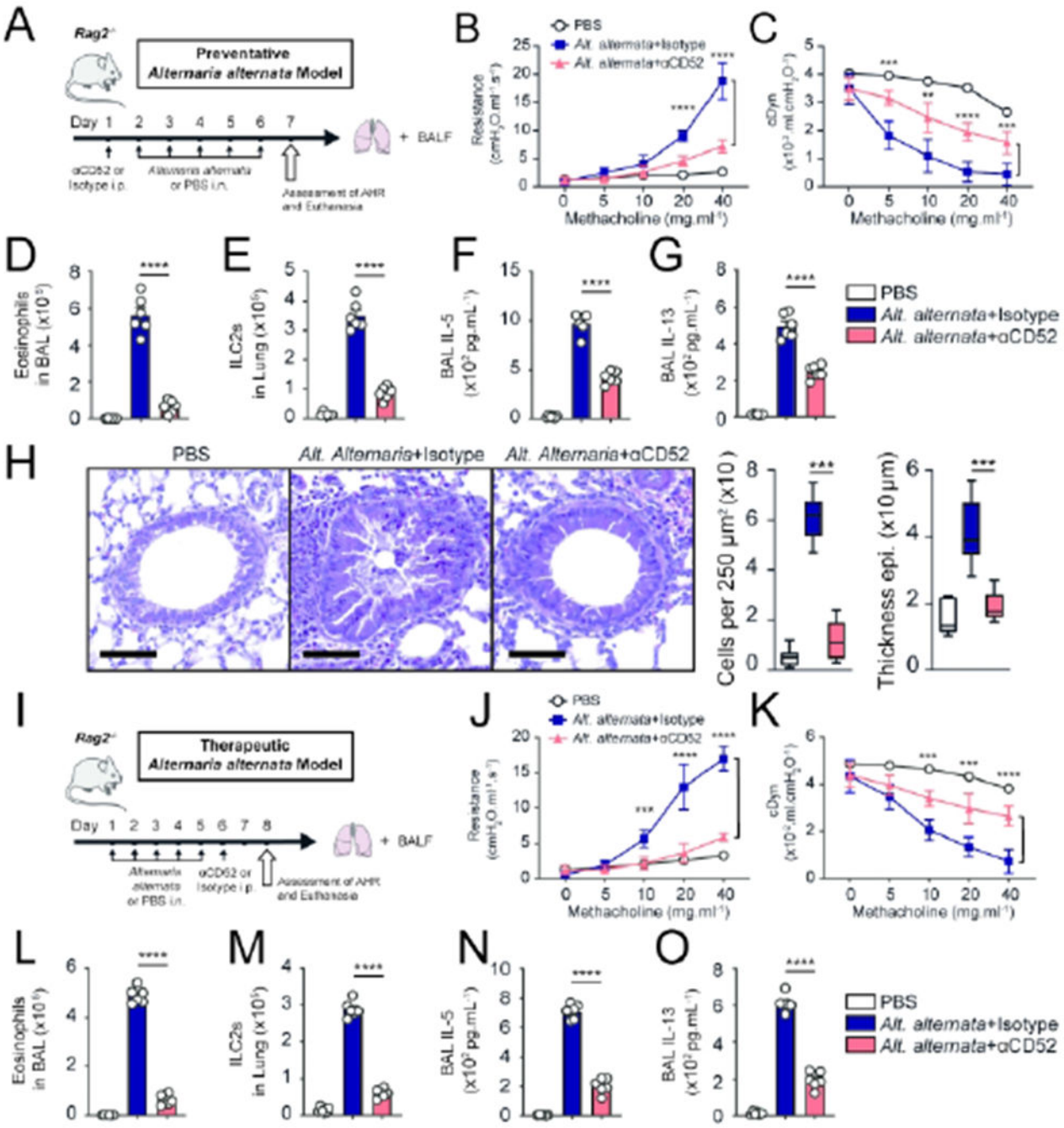

Figure 4. CD52 depletion ameliorates *Alternaria alternata*-induced AHR.

A, A group of *Rag2*$^{-/-}$ mice (n=6 mice) were treated with 250µg of anti-CD52 depleting antibody (αCD52) *i.p.* or isotype control on day 1. The mice were then challenged with *Alternaria alternata* (100 µg in 50 µL) or PBS intranasally *(i.n.)* on days 2 to 6. On day 7, we assessed the lung function, as shown in the timeline. **B** and **C,** Line graph show lung resistance and dynamic compliance (cDyn) in response to increasing doses of methacholine. **D,** the numbers of eosinophils in the BAL. **E,** the numbers of ILC2s in the lungs. **F** and **G**, bar graph show secretion levels of IL-5 and IL-13 in BAL. **H,** Representative images (left

panel) and quantification (right panel) of hematoxylin and eosin–stained histologic sections of the lungs of mice. Scale bars=50 μm. I, A group of *Rag2*$^{-/-}$ mice (n=6 mice) were challenged with *Alternaria alternata* (100 μg in 50 μL) or PBS intranasally *(i.n.)* on days 1 to 5. On day 6, the mice were treated with 250μg of αCD52 *i.p.* or isotype control. The lung function and samples were measured on day 8. **J,** lung resistance. **K,** dynamic compliance. **L,** number of eosinophils in BAL fluid. **M,** number of ILC2s in lungs. **N** and **O**, BAL IL-5 and IL13 levels. Data are shown as means ± SEMs and are representative of 3 individual experiments. Statistical analysis, two-tailed student's t-test; **P < .01, ***P < .001, ****P < .0001. Mouse and lung images are provided with permission from Servier Medical Art.

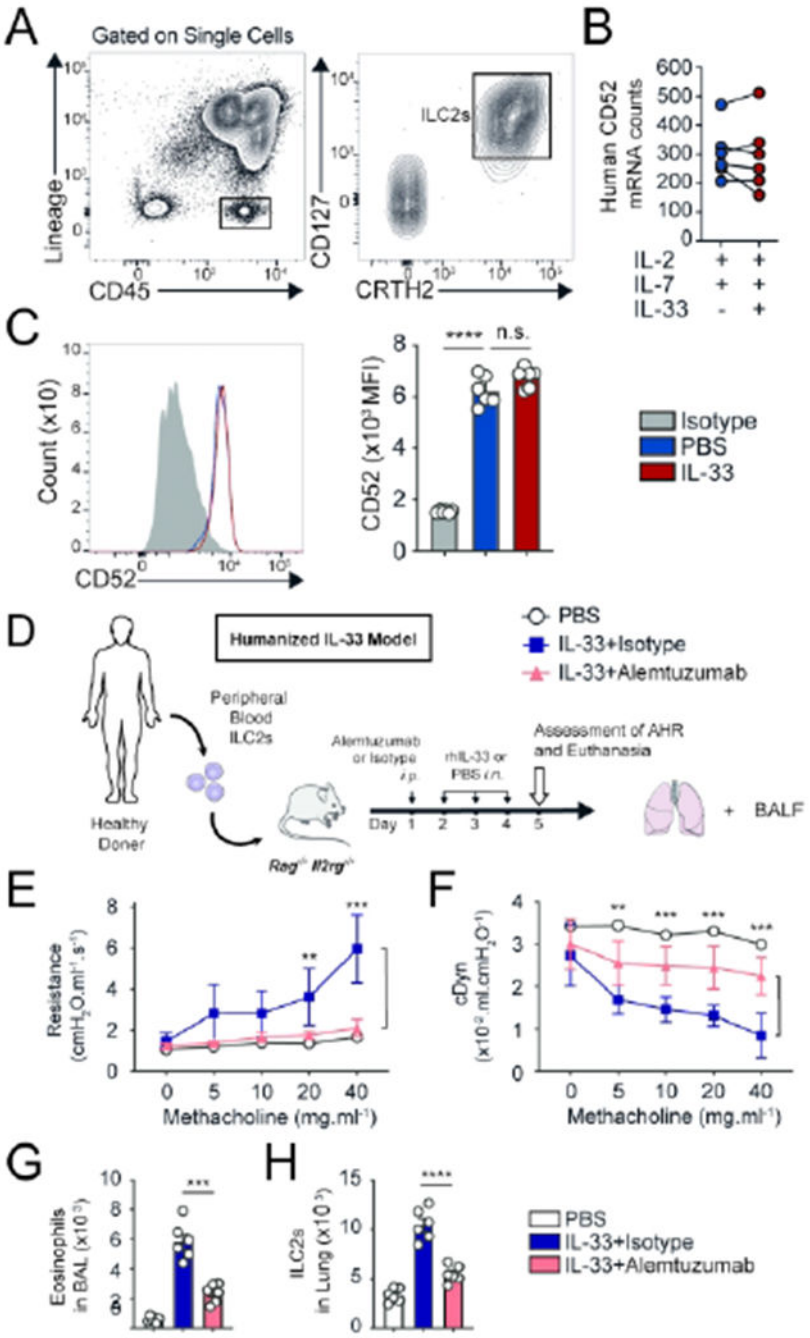

Figure 5. Human ILC2s express CD52, and Alemtuzumab ameliorates human ILC2-mediated AHR.

Human peripheral-blood ILC2s were freshly sorted (n=6 donors) and cultured with 10 ng of recombinant human (rh)-IL-2 and rh-IL-7 in presence or absence of rh-IL-33 (10 ng). CD52 mRNA expression levels were analyzed after 9 hours and CD52 protein expression levels were analyzed after 48 hours. **A,** the gating strategy of human ILC2s identified as Lin^{-} $CD45^{+}CD127^{+}CRTH2^{+}$ cells. **B** and **C,** Expression levels of CD52 at a mRNA and protein levels in both naive (PBS) and IL-33-activated human ILC2s. Corresponding quantitation of

CD52 expression shown as MFI+/− SEM, n = 6. **D,** human peripheral ILC2s (n=6 donors) were purified via FACS and cultured with recombinant human (rh)-IL-2 (20 ng/ml) and rh-IL-7 (20 ng/ml) for 48 hours, and then adoptively transferred into *Rag2*$^{-/-}$*Il2rd*$^{-/-}$ mice that were treated with 250μg of Alemtuzumab *i.p.* or isotype control on day 1. Additionally, mice were challenged with either rh-IL-33 (1 μg) or PBS intranasally (*i.n.*) on days 2, 3 and 4. Measurement of lung function and analysis of BAL followed on day 5, as shown in the timeline. **E** and **F,** Line graph show lung resistance and dynamic compliance (cDyn) in response to increasing doses of methacholine. **G,** the numbers of eosinophils in the BAL. **H,** the numbers of human ILC2s in the lungs. Data are shown as means ± SEMs and are representative of 3 individual experiments. Statistical analysis, two-tailed student's t-test or one-way ANOVA followed by Tukey post-hoc tests; *P < .05, **P < .01, ***P < .001, ****p < .0001, and n.s., non-significant. Human, mouse and lung images are provided with permission from Servier Medical Art.

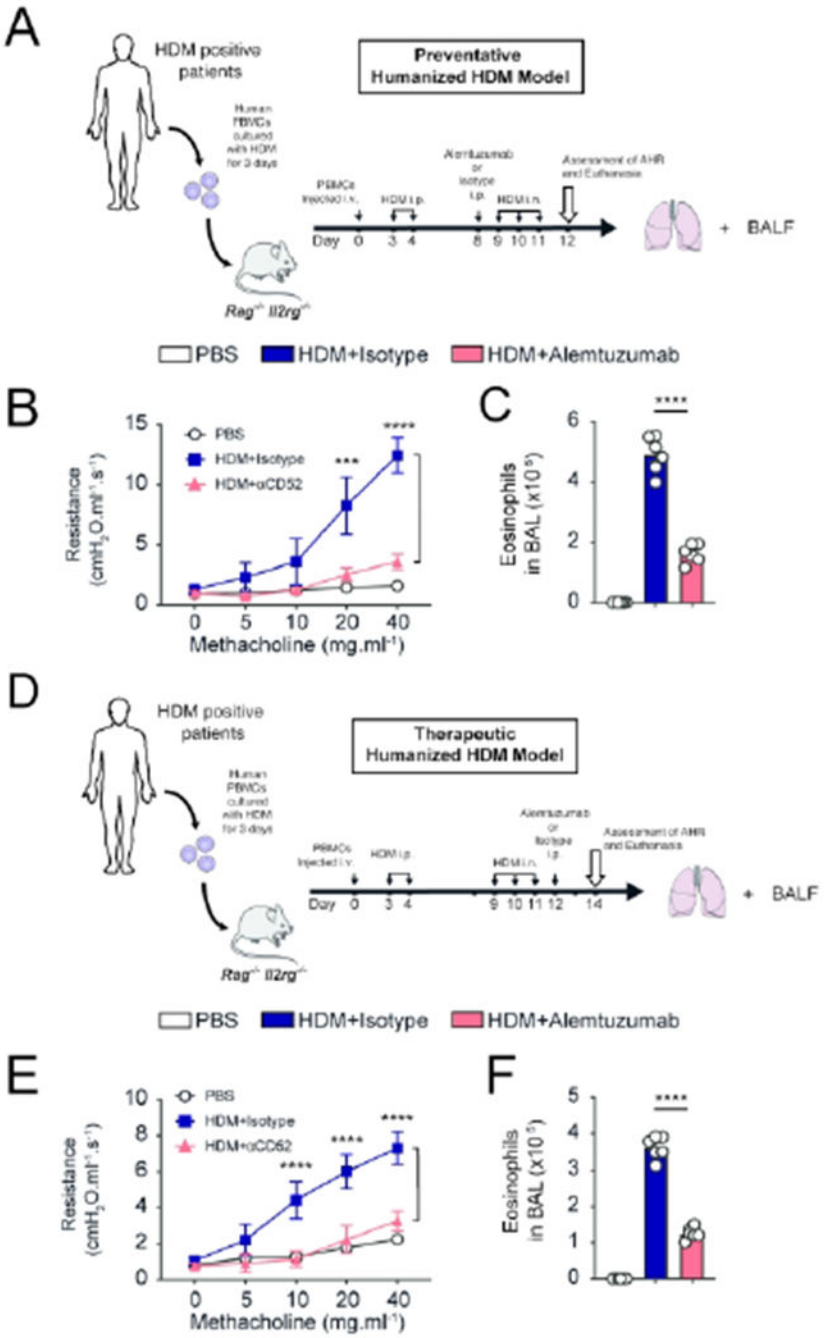

Figure 6. Alemtuzumab ameliorates HDM-induced AHR in preventative and therapeutic humanized mice models.

A, Total PBMCs from HDM positive patients (5 million) were adoptively intravenously transferred into *Rag2*$^{-/-}$*Il2rg*$^{-/-}$ mice that were sensitized on days 3 and 4 (n=6 donors). At day 8, mice received an intraperitoneal injection of Alemtuzumab or control isotype (250μg). Subsequently, the humanized mice were challenges with HDM (50μg) or PBS i.n. on days 9, 10 and 11. Measurement of lung function and inflammation were performed on day 14. **B,** lung resistance measured in anesthetized, tracheostomized, and mechanically

ventilated mice that were exposed to increasing concentrations of methacholine. **C**, number of eosinophils in BAL. **D,** 5 million total PBMCs from HDM positive patients (n=6 donors) were adoptively intravenously transferred into *Rag2*$^{-/-}$*Il2rg*$^{-/-}$ mice that were then sensitized on days 3 and 4. The humanized mice were then challenges with HDM (50μg) or PBS i.n. on days 9, 10 and 11. On day 12, mice received an intraperitoneal injection of Alemtuzumab or control isotype (250μg). Measurement of lung function and inflammation were performed on day 14. **E,** lung resistance. **F,** number of eosinophils in BAL. Statistical analysis, two-tailed student's t-test; ***P < .001, and ****p < .0001. Human, mouse and lung images are provided with permission from Servier Medical Art.